Anal. Chem. **2005,** *77,* 3979−3985

Detection and Quantification of On-Chip Phosphorylated Peptides by Surface Plasmon Resonance Imaging Techniques Using a Phosphate Capture Molecule

Kazuki Inamori,[†] Motoki Kyo,[†] Yoshiaki Nishiya,[†] Yusuke Inoue,[‡] Tatsuhiko Sonoda,[‡] Eiji Kinoshita,[§] Tohru Koike,[§] and Yoshiki Katayama*[,‡]

Biotechnology Frontier Project, Toyobo Co., Ltd., 10-24 Toyo-cho, Tsuruga, Fukui 914-0047, Japan, Department of Applied Chemistry Faculty of Engineering, Kyushu University, 6-10-1 Hakozaki Higashi-ku, Fukuoka 812-8581, Japan, and Department of Functional Molecular Science, Division of Medicinal Chemistry, Graduate School of Biomedical Sciences, Hiroshima University, 1-2-3 Kasumi Minami-ku, Hiroshima 734-8551, Japan

We describe herein a detection and quantification system for on-chip phosphorylation of peptides by surface plasmon resonance (SPR) imaging techniques using a newly synthesized phosphate capture molecule (i.e., biotinylated zinc(II) complex). The biotinylated compound is a dinuclear zinc(II) complex that is suitable for accessing phosphate anions as a bridging ligand on the two zinc(II) ions. The compound was exposed on the peptide array and detected with streptavidin (SA) via a biotin−SA interaction by SPR imaging. In the conventional method using antibody, both anti-phosphoserine and anti-phosphotyrosine antibodies were required for phosphoserine and phosphotyrosine detection, respectively. Detection of the phosphate group by the zinc(II) complex, however, was independent of the phosphorylated amino acid residues. The calibration curve for the phosphorylation ratios was established with a calibration chip, on which phosphoserine-containing peptide probes were immobilized. The peptide probes, which were phosphorylated on the surface by protein kinase A, were detected and quantified by SPR imaging using the zinc(II) complex, SA, and anti-SA antibody. The reaction rate and the kinetics of on-chip phosphorylation were also evaluated with the peptide array. The phosphorylation ratio was saturated at ~20% in 2 h in this study.

Phosphorylation of proteins by protein kinases plays a crucial role in intracellular signal transduction systems. To analyze kinase activity or kinase expression, peptide probes have been commonly used as substrates of kinases, and many peptide substrates have been screened for these kinase assays.[1] By conventional methods, phosphorylation reactions are carried out in solution and are detected by radioisotope scintillation,[2] ELISA,[3,4] or mass spectrometry.[5] But these methods are low-throughput and usually require laborious procedures.

In the past decade, "chip" technology, which can study various interactions using microarrays, has progressed significantly and has been established as essential to high-throughput analysis.[6] In addition, many researchers have carried out phosphorylation assays with immobilized substrates on glass slides[7−15] or membranes.[16] The on-chip phosphorylations are detected using autoradiography with [γ-^{32}P/^{33}P]-ATP[7−10,16] or a fluorescent scanner with labeled anti-phospho (amino acid) antibodies.[12−15] Although these detection methods are sensitive, it has been difficult to quantify the phosphorylation reactions.

We describe herein the detection and quantification of on-chip phosphorylation by a surface plasmon resonance (SPR) technique, which is known as a semiquantitative analytical method. In

* To whom correspondence should be addressed. Phone: +81-92-642-3608. Fax: +81-92-642-3606. E-mail: ykatatcm@mbox.nc.kyushu-u.ac.jp.

[†] Toyobo Co. Ltd.

[‡] Kyushu University.

[§] Hiroshima University.

(1) Sills, M. A.; Weiss, D.; Pham, Q.; Schweitzer, R.; Wu, X.; Wu, J. J. *J. Biomol. Screening* **2002**, *7*, 191−214.

(2) Till, J. H.; Annan, R. S.; Carr, S. A.; Miller W. T. *J. Biol. Chem.* **1994**, *269*, 7423−7428.

(3) Lehel, C.; Daniel-Issakani, S.; Brasseur, M.; Strulovici, B. *Anal. Biochem.* **1997**, *244*, 340−346.

(4) Ross, H.; Armstrong, C. G.; Cohen, P. *Biochem. J.* **2002**, *366*, 977−981.

(5) Sonoda, T.; Shigaki, S.; Nagashima, T. Okitsu, O.; Kita, Y.; Murata, M.; Katayama, Y. *Bioorg. Med. Chem. Lett.* **2004**, *14*, 847−850.

(6) Schena, M.; Shalon, D.; Davis, R. W.; Brown, P. O. *Science* **1995**, *270*, 467−470.

(7) MacBeath, G.; Schreiber, S. L. *Science* **2000**, *289*, 1760−1763.

(8) Williams, D. M.; Cole, P. A. *Trends Biochem. Sci.* **2001**, *26*, 271−273.

(9) Falsey, J. R.; Renil, M.; Park, S.; Li, S.; Lam, K. S. *Bioconjugate Chem.* **2001**, *12*, 346−353.

(10) Zhu, H.; Klemic, J. F.; Chang, S.; Bertone, P.; Casamayor, A.; Klemic, K. G.; Smith, D.; Gerstein, M.; Reed, M. A.; Snyder, M. *Nat. Genet.* **2002**, *26*, 283−289.

(11) Lizcano, J. M.; Deak, M.; Morrice, N.; Kieloch, A.; Hastie C. J.; Dong, L.; Schutkowski, M.; Reimer, U.; Alessi, D. R. *J. Biol. Chem.* **2002**, *277*, 27839−27849.

(12) Reimer, U.; Reineke, U.; Schneider-Mergener, J. *Curr. Opin. Biotechnol.* **2002**, *13*, 315−320.

(13) Lesaicherre, M. L.; Uttamchandani, M.; Chen, G. Y. J.; Yao, S. Q. *Bioorg. Med. Chem. Lett.* **2002**, *12*, 2079−2083.

(14) Lesaicherre, M. L.; Uttamchandani, M.; Chen, G. Y. J.; Yao, S. Q. *Bioorg. Med. Chem. Lett.* **2002**, *12*, 2085−2088.

(15) Chen, G. Y. J.; Uttamchandani, M.; Lue, R. Y. P.; Lesaicherre, M. L.; Yao, S. Q. *Curr. Top. Med. Chem.* **2003**, *3*, 705−724.

(16) Schutkowski, M.; Reimer, U.; Panse, S.; Dong, L.; Lizcano, J. M.; Alessi, D. R.; Schneider-Mergener, J. *Angew. Chem.* **2004**, *43*, 2671−2674.

10.1021/ac050135t CCC: $30.25
Published on Web 05/11/2005

particular, we applied the SPR imaging technique, which can observe multiple interactions with an array format,[17,18] to analyze the multiple peptide probes immobilized on the chip.

The on-chip phosphorylation cannot be detected directly by SPR, which observes the refractive index change on a gold surface, because the increase in molecular weight by phosphorylation is too small. It is therefore essential for SPR assays to use detection reagents, which can specifically bind to phosphate groups.

Recently, an SPR detection system with anti-phosphotyrosine antibody has been proposed.[19] The antibodies, whose epitopes are phosphoserine/threonine/tyrosine, are commercially available and can be applied to phosphorylation detection on SPR. However, multiple antibodies are required for the peptide array, on which many kinase substrates are immobilized.

For phosphate group recognition, we have investigated the zinc(II) chelate compound[20−24] and have reported its application to mass spectrometry analysis.[25] The chelate compound can bind to the phosphate group regardless of the species of the phosphorylated amino acid residue. In this study, the chelate compound was applied to the SPR imaging technique to detect the phosphorylated peptide probe on the gold surface. A novel biotinylated zinc(II) chelate compound was synthesized, exposed on the peptide array, and then detected with streptavidin (SA) via a biotin−SA interaction.

To quantify the phosphorylation, the calibration chip was fabricated with a phosphorylated peptide probe containing phosphoserine. The calibration curve for the phosphorylation ratios was established using the chelate compound, SA, and anti-SA antibody (anti-SA) in the SPR imaging measurement. The reaction rates and kinetics of on-chip phosphorylations by protein kinase A (PKA) were investigated. Our established assay was useful for evaluating the phosphorylation on a peptide chip. This technique should be suitable for kinase activity assays and kinase expression profiling.

EXPERIMENTAL SECTION

Materials. Sulfosuccinimidyl-4-(*N*-maleimidomethyl) cyclohexane-1-carboxalate (SSMCC, Pierce), thiol-terminated methoxypoly(ethylene glycol) MW 5000 (PEG-thiol, NOF), cAMP-dependent protein kinase catalytic subunit (PKA, Promega), adenosine 5′-triphosphete disodium salt hydrate (ATP, Sigma-Aldrich), [γ-^{32}P]ATP (Amersham), SA (Molecular Probes), anti-SA (Vector), anti-phosphoserine antibody (anti-pSer, PSR-45, Sigma-Aldrich), anti-phosphotyrosine antibody (anti-pTyr PT-66, Sigma-Aldrich), *N*-succuinimidyl D-biotinate (Sigma-Aldrich), and *N*-(5-(2-aminoethylcarbamoyl)pyridin-2-ylmethyl)-*N*,*N*′,*N*′-tris-(pyridin-2-ylmethyl)-1,3-diaminopropan-2-ol (Nard Institute), the molecular structure of which is shown in Figure 1, were used without further purification. The other reagents and solvents used were of analytical quality. All aqueous solutions were prepared with deionized and distilled water.

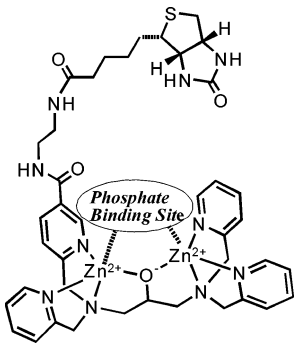

Figure 1. Molecular structure of a novel zinc(II) compound, biotinylated Zn_2L^{3+}, which can form the chelate complex with a phosphate group.

Synthesis of Biotinylated Zinc(II) Chelate Compound. *N*-Succuinimidyl D-biotinate was allowed to react with *N*-(5-(2-aminoethylcarbamoyl)pyridin-2-ylmethyl)-*N*,*N*′,*N*′-tris(pyridin-2-ylmethyl)-1,3-diaminopropan-2-ol to obtain a biotinylated zinc(II) chelate compound (biotinylated ligand, HL). Thus, a DMF solution (10 mL) of *N*-succuinimidyl D-biotinate (0.33 g, 0.96 mmol) was added to a DMF solution (5 mL) of *N*-(5-(2-aminoethylcarbamoyl)-pyridin-2-ylmethyl)-*N*,*N*′,*N*′-tris(pyridin-2-ylmethyl)-1,3-diaminopropan-2-ol (0.51 g, 0.95 mmol) at 0 °C. After the mixture was allowed to stand at room temperature for 2 h, the solvent was evaporated. The yellowish residue was purified by silica gel column chromatography (eluent, $CHCl_3$:MeOH = 20:1) to obtain *N*-(5-(2-(+)-biotinaminoethylcarbamoyl)pyridin-2-ylmethyl)-*N*,*N*′,*N*′- tris(pyridin-2-ylmethyl)-1,3-diaminopropan-2-ol (HL) as a brown solid (0.54 g, 74% yield). Thin-layer and column chromatography were performed using a silica gel TLC plate (5554, Merck) and NH-DM 1020 silica gel (Fuji Silisia Chemical), respectively. TLC (eluent, CH_3CN:MeOH:28% aqueous NH_3 = 20:5:3) R_f = 0.65.

The synthesized ligand, HL, was characterized by IR, ^{1}H NMR, ^{13}C NMR, and MALDI-TOF MS. An IR spectrum was recorded on an infrared spectrometer (FT-710, Horiba) with a KCl pellet at 20 ± 2 °C. In the NMR study, ^{1}H (500 MHz) and ^{13}C (125 MHz) NMR spectra at 35.0 ± 0.1 °C were measured on a LA500 spectrometer (JEOL). Tetramethylsilane (in $CDCl_3$) was used as an internal reference for ^{1}H and ^{13}C NMR measurements. MALDI-TOF MS spectra (positive reflector mode) were obtained on a BioSpectrometry Workstation (Voyager RP-3, PerSeptive Biosystems) equipped with a nitrogen laser (337 nm, 3-ns pulse). The time-to-mass conversion was achieved by external calibrations using peaks for α-cyano-4-hydroxycinnamic acid (m/z 190.05 for M + H^+ and m/z 212.03 for M + Na^+) and a peptide, Ac−Ile-Tyr-Gly-Glu-Phe-NH_2 (m/z 691.31 for M + Na^+).

Characterization of Biotinylated Ligand and Its Zinc(II) Complex. The analysis results of IR, ^{1}H NMR, ^{13}C NMR, and MALDI-TOF MS were as follows. Mass spectrometry measurement was carried out due to the confirmation of the formation of the desired complex (1:2 complex). IR (cm^{-1}): 3290, 3064, 2928,

(17) Nelson, B. P.; Frutos, A. G.; Brockman, J. M.; Corn, R. M. *Anal. Chem.* **1999**, *71*, 3928−3934.
(18) Brockman, J. M.; Nelson, B. P.; Corn, R. M. *Annu. Rev. Phys. Chem.* **2000**, *51*, 41−63.
(19) Houseman, B. T.; Huh, J. H.; Kron, S. J.; Mrksich, M. *Nat. Biotechnol.* **2002**, *20*, 270−274
(20) Ojida, A.; Mito-oka, Y.; Inoue, M.; Hamachi I. *J. Am. Chem. Soc.* **2002**, *124*, 6256−6258.
(21) Koike, T.; Inoue, M.; Kimura, E.; Shiro, M. *J. Am. Chem. Soc.* **1996**, *118*, 3091−3099.
(22) Kimura, E.; Aoki, S.; Koike, T.; Shiro, M. J. *Am. Chem. Soc.* **1997**, *119*, 3068−3076.
(23) Fujioka, H.; Koike, T.; Yamada, N.; Kimura, E. *Heterocycles* **1996**, *42*, 775−787.
(24) Kinoshita, E.; Takahashi, M.; Takeda, H.; Shiro, M.; Koike, T. *Dalton Trans.* **2004**, *8*, 1189−1193.
(25) Takeda, H.; Kawasaki, A.; Takahashi, M.; Yamada, A.; Koike, T. *Rapid Commun. Mass Spectrom* **2003**, *17*, 2075−2081.

Table 1. Peptide Sequences of Surface-Immobilized Probes

probe	kinase	peptide sequence	comment
1	PKA	CGGLRRASLG-NH_2	
2	PKA	CGGLRRAĀLG-NH_2	Ala-substituted
3	PKA	CGGLRRAS̄(PO_3)LG-NH_2	Ser-phosphorylated
4	c-Src	CGIYG EFK$\overline{KK}$−NH_2	
5	c-Src	CGIȲ(PO_3) G EFKKK−NH_2	Tyr-phosphorylated

2824, 1701, 1647, 1595, 1570, 1546, 1476, 1435, 1367, 1328, 1265, 1244, 1150, 1121, 1049, 1003, 858, 766. ^{1}H NMR ($CDCl_3$): δ 1.28−1.48 (2H, m, CCH_2C), 1.48−1.73 (4H, m, CCH_2C), 2.10−2.28 (2H, m, CCH_2CO), 2.50−2.78 (5H, m, NCH_2CCH_2N and SCHC), 2.78−1.90 (1H, m, SCHC), 2.98−3.10 (1H, m, SCHC), 3.38−3.75 (4H, m, NCH_2CH_2N), 3.82−3.40 (9H, m, NCH_2Py and NCCHCN), 4.19−4.28 (1H, m, NCHCS), 4.38−4.48 (1H, m, NCHCS), 5.92 (1H, s, HN), 6.64 (1H, bs, HN), 7.07−7.18 (3H, m, PyH), 7.31−7.38 (3H, m, PyH), 7.44 (1H, d, PyH), 7.59 (3H, ddd, PyH), 8.03 (1H, dd, PyH), 8.15 (1H, bs, NHCO), 8.40−8.55 (3H, m, PyH), 8.94 (1H, d, PyH). ^{13}C NMR ($CDCl_3$): δ 25.4, 28.0, 35.7, 39.5, 40.6, 41.0, 55.6, 59.2, 60.3, 60.7, 60.8, 61.0, 61.8, 67.4, 122.1, 122.7, 123.2, 128.3, 135.5, 136.5, 148.0, 149.0, 159.3, 159.4, 162.7, 164.2, 166.5, 174.9. MALDI-TOF MS: zinc(II)-free ligand (HL) in a 50% (v/v) CH_3CN solution containing α-cyano-4-hydroxycinnamic acid (10 mg/mL); m/z 767.4 for M + H^+.

Since all attempts failed to isolate the zinc(II) complex (Zn_2L^{3+}) with the biotinylated ligand (an alkoxide form, L), *N*-(5-(2-(+)-biotinaminoethylcarbamoyl)pyridin-2-ylmethyl)-*N*,*N*′,*N*′-tris-(pyridin-2-ylmethyl)-1,3-diaminopropan-2-ol, a phosphate-bound zinc(II) complex ($[Zn_2L_{3+}-HOPO_3^{2-}]^+$), was proven by MALDI-TOF MS from a mixture of 2 mM $Zn(CH_3COO)_2$, 1 mM HL, and 12.5 mM NaH_2PO_4−NaOH (pH 6.9) in a 50% (v/v) CH_3CN solution containing 2,4,6-trihydroxyacetophenone (10 mg/mL): m/z 989.2. An analogous zinc(II) complex, *N*,*N*′,*N*′-tetrakis(pyridine-2-ylmethyl)-1,3-diaminopropan-2-olate dizinc(II) complex, was reported as a phosphate capture molecule (K_d = 25 nM for phenyl phosphate dianion), which was characterized by MALDI TOF-MS analysis and X-ray crystallography.[24]

Peptide Preparation. All peptides used in this study and shown in Table 1 were synthesized by a peptide synthesizer (Pioneer, Applied Biosystems) and purified by HPLC (BioCAD perfusion chromatography system, Applied Biosystems) using an ODS-A column with a 12-nm pore size (YMC). Kemptide peptide,[26] to which cysteine and two glycine residues were attached at the C terminus, was used as a PKA substrate (probe 1). We prepared the negative control of Kemptide (probe 2), on which the serine is substituted with alanine, and the positive control (probe 3), which has a phosphoserine residue. The substrate of c-Src kinase[19] (probe 4) and its positive control (probe 5) were also synthesized to determine the reaction specificity of PKA.

Fabrication of Peptide Arrays. The covalently immobilized peptide array was obtained by a modified procedure, which was reported on DNA array.[27] Briefly, a patterned amino-modified Au-coated chip (Toyobo), which has amino groups in 96 areas with a 500-μm square and PEG background, was allowed to react for 30 min with 300 μL of 1 mM SSMCC to create a maleimido-modified surface. Next, 10-nL drops of 1 mg/mL cysteine-terminated peptide substrates were delivered automatically on the maleimido surface using an automated spotter (Toyobo), and the maleimido−thiol reaction was carried out overnight. A300-μL aliquot of 10 mg/mL PEG-thiol were reacted on the peptide array for 30 min to block the unreacted maleimido group. The surface was then rinsed with phosphate buffer and water. A phosphate buffer (10 mM phosphate, pH 7.2, and 150 mM NaCl) was used for all reactions in array fabrications.

On-Chip Phosphorylation. The peptide arrays were reacted at 30 °C with 400 μL of 0.2 unit/μL PKA solution in reacting buffer (50 mM Tris-HCl, 50 mM $MgCl_2$, pH 7.4) containing 10 μM ATP. For the autoradiography assay, 5000 Ci/mmol [γ-^{32}P]-ATP was used instead of ATP. After the reactions, the arrays were rinsed with PBS and MilliQ water, and then dried with air flow.

SPR Imaging Analysis. (i) Detection with Antibody. The peptide array was placed into an SPR imaging instrument (Toyobo). The running buffer for the antibody (50 mM Tris-HCl, pH 7.4) was applied to the array surface at 100 μL/min. The array surface was treated with 1 μg/mL antibody solution in the running buffer for 10 min and then rinsed with the running buffer for 10 min. The signal data were collected with the SPR analysis program (Toyobo). All SPR experiments were performed at 30 °C.

(ii) Detection with Biotinylated Zn_2L^{3+} and SA. A 300-μL aliquot of 2 μg/mL biotinylated Zn_2L^{3+} solution, which was dissolved in the buffer (10 mM HEPES−NaOH, 0.2 M sodium nitrate, 1 mM zinc nitrate, 0.005% (w/v) Tween 20, 10% ethanol, pH 7.4), was poured on the peptide array and incubated for 30 min at room temperature. The array was then immediately placed on the SPR instrument and exposed by 1 μg/mL SA solution in the running buffer (10 mM HEPES−NaOH, pH 7.4) for 10 min and then rinsed with the running buffer for 5 min. For the quantification of phosphorylation, 1 μg/mL anti-SA solution in the running buffer was injected subsequently for 20 min into the SPR imaging instrument to enhance the signals. The SPR difference image was constructed using Scion Image (Scion).

Autoradiography Experiment. The array was reacted with [γ-^{32}P]-ATP and exposed to SG imaging plates (Fuji Photo Film) for 30 min. The plates were observed with an imaging analyzer (BAS-1800 II; Fuji Photo Film). The obtained images were processed using PhotoShop (Adobe).

RESULTS AND DISCUSSION

Strategy of Phosphorylation Detection. The strategy for phosphorylation detection of the fabricated peptide arrays is summarized in Figure 2. Phosphate groups were created on the chip surface by an on-chip phosphorylation reaction or an immobilization of phosphoserine/tyrosine-containing peptides. We evaluated three different schemes for phosphorylation detection, as follows. In scheme A, the phosphate groups were detected with antibodies, anti-phosphoserine/tyrosine antibody with SPR.[19] In scheme B, the phosphate groups on the chip surface formed a phosphate-bound complex with biotinylated zinc(II) complex (Zn_2L^{3+}), the molecular structure of which is shown in Figure 2. Subsequently, the chip was placed into the SPR imaging instrument and exposed by SA. The interactions between Zn_2L^{3+} and SA were detected using SPR imaging. The on-chip phosphoryla-

(26) Kemp, B. E.; Graves, D. J.; Benjamini, E.; Krebs, E. G. *J. Biol. Chem.* **1977**, *252*, 4888−4894.

(27) Kyo, M.; Yamamoto, T.; Motohashi, H.; Kamiya, T.; Kuroita, T.; Tanaka, T.; Engel, J. D.; Kawakami, B.; Yamamoto, M. *Genes Cells* **2004**, *9*, 153−164.

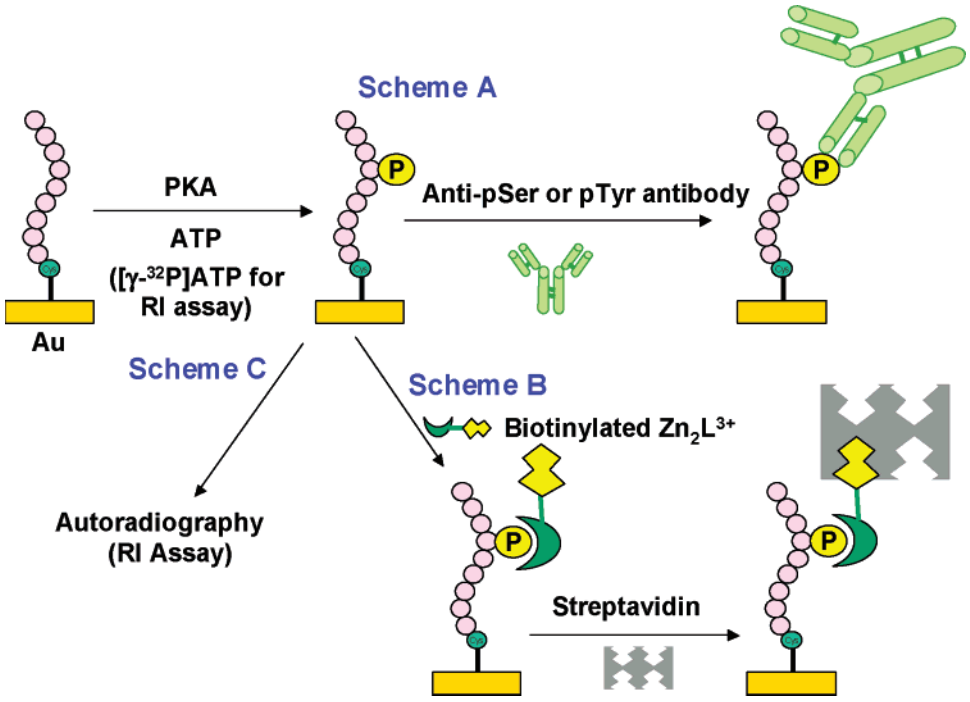

Figure 2. Strategy of phosphorylation detection of immobilized substrate peptide. Scheme A: The binding of anti-phosphoserine/-tyrosine antibody to phosphorylated amino acid residue on peptide probe was observed by SPR imaging. Scheme B: A novel zinc(II) compound, biotinylated Zn_2L^{3+}, bound to the phosphate group of the peptide probe. The streptavidin binding was monitored by SPR imaging. Scheme C: Autoradiography detected the ^{32}P uptake by on-chip phosphorylation with PKA and [$\gamma-^{32}P$] ATP.

tions were also directly observed using a radioisotope ([γ-^{32}P]-ATP) and autoradiography (scheme C).

In this study, we have demonstrated the advantages of our proposed system (scheme B) compared to the established method (scheme A). RI detection (scheme C) was studied to verify ATP uptake by on-chip phosphorylation.

Detection of Phosphoserine/-Tyrosine-Containing Peptides with Antibody by SPR Imaging (Scheme A). A peptide array with probes 1−5 was fabricated for this analysis. The peptide array was placed on an SPR imaging instrument and exposed by anti-pTyr and anti-pSer in sequence. The SPR signal changes are shown in Figure 3. The SPR signal on probe 5 was increased by the anti-pTyr exposure, indicating that anti-pTyr bound specifically to the phosphotyrosine on probe 5. The phosphoserine on probe 3 was recognized by anti-pSer. In this way, antibodies could bind to the phosphorylated amino acid residue. However, multiple antibodies are required for the various phosphorylation analyses. Furthermore, the antibodies might be lacking a specificity to phosphoserine, as seen with probe 5 in Figure 3.

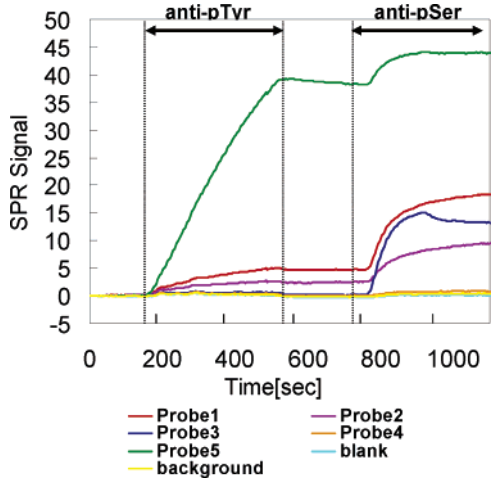

Figure 3. SPR signal changes by anti-phosphoserine and anti-phosphotyrosine antibody injection to the SPR imaging instrument. The peptide array was exposed with antibody for 5 min and then rinsed for 3 min.

Detection of Phosphoserine/-Tyrosine-Containing Peptides with Biotinylated Zinc(II) Complex by SPR Imaging (Scheme B). For this study, probes 1−5, which are shown in Table 1, were immobilized on the chip. We tried to detect probes 3 and 5, both of which contain phosphoserine and phosphotyrosine, respectively, with biotinylated Zn_2L^{3+} by an SPR imaging technique. The fabricated array was exposed with the Zn_2L^{3+} solution, and we then analyzed the interaction between biotin and SA by SPR imaging.

The SPR results are shown in Figure 4. Sharp increases in the SPR signals were observed for the phosphoserine-tyrosine-containing peptides (probes 3 and 5). The signal changes in peptides that did not contain the phosphoamino acid residue were negligible. Furthermore, there were no nonspecific bindings to the PEG background and to the blank spot, both of which were modified with SSMCC and blocked with PEG-thiol. We therefore believe that the signal increases for probes 3 and 5 were specific to the phosphorylated peptides.

The advantage of this system is that either phosphoserine or phosphotyrosine can be detected by a single probe complex; a Zn_2L^{3+} can form a complex with only the phosphate moiety on the peptide. On the other hand, a conventional antibody-detecting system needs multiple antibodies because the antibodies bind not just to the phosphate group itself but also to the phosphoamino acid residues.

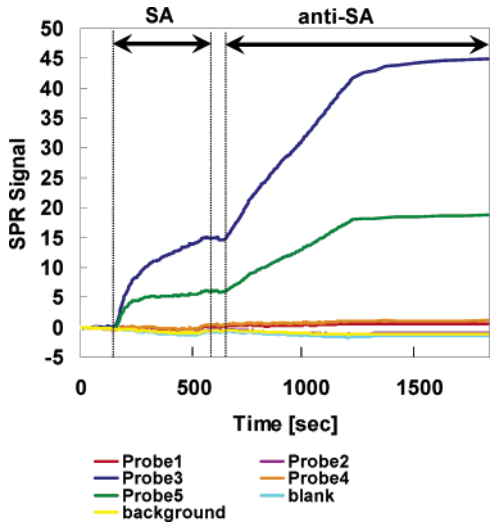

Figure 4. SPR analysis by exposure of SA and anti-SA on the peptide array, which was pretreated with biotinylated Zn_2L^{3+}.

In this study, a signal difference between probes 3 and 5 was observed. Both probes should have been 100% phosphorylated because the probes were synthesized using phosphoserine/-tyrosine by a solid-phase peptide synthesis method. The immobilized densities of the peptides were considered to not differ significantly because the SPR angles of the spots and the brightness of the spots at the measurement angle were almost the same (data not shown). The signal difference in the SPR measurement implies that the peptide sequences may affect the signal. We have not yet identified whether the phosphate−Zn_2L^{3+} interaction or the Zn_2L^{3+}−SA interaction caused the difference.

Moreover, the SPR signals by SA could be enhanced with anti-SA, as the anti-SA molecule is large enough to affect the refractive index near the gold surface. The anti-SA selectively bound to the probe 3 and 5 spots, on which SA had already interacted (Figure 4). Note that negligible signal changes were observed on probes 1 and 4, the blank, and background. Moreover, the repeat exposure of SA and biotinylated anti-SA to the array was found to amplify the signal. By this strategy, we expect that the detection sensitivity of peptide phosphorylation can be greatly improved.

Quantification of Immobilized PhosphoSerine-Containing Peptides. Generally, the reaction rate by protein kinase cannot be 100%. We therefore fabricated a peptide array on which a mixture of 100% phosphorylated and 0% phosphorylated peptides was immobilized in various mixing ratios. The phosphate groups were then detected with Zn_2L^{3+}, SA, and anti-SA by SPR imaging. The magnitudes of the SPR signals in response to the exposure of SA and anti-SA were evaluated to quantify the phosphorylation percent.

Thus, mixture solutions of probes 1 and 3 at various mixture ratios were prepared and spotted on the chip to fabricate a calibration array. Immobilized peptides were "pseudo"-phosphorylated at various ratios according to the hypothesis that the reactivity of probe 1 to the maleimido surface was equal to that of probe 3.

The SPR difference image, which was obtained by an exposure of 1 μg/mL SA, is shown in Figure 5A. The array pattern is described in Figure 5B, in which brilliant gradations of SPR signals can be observed. The signal ratios of each spot to the 100% phosphorylated spot were calculated to establish the calibration curve, as the intensities of the SPR signals for 100% phosphorylated lacked reproducibility. We found the signal ratios for the spots to show acceptable reproducibility for the calibration curve, which is shown in Figure 5C. The horizontal axis is the phosphorylation percent, which is, in fact, the mixing ratio of probes 1 and 3. The vertical axis is the ratio between the obtained signals at the mixture ratios and that of probe 3. Figure 5C indicates that the SPR signal ratio corresponds to the phosphorylation ratio on the chip. In the case of this study with probe 1, the intensity of the SPR signal was saturated at ~40% phosphorylation. A similar

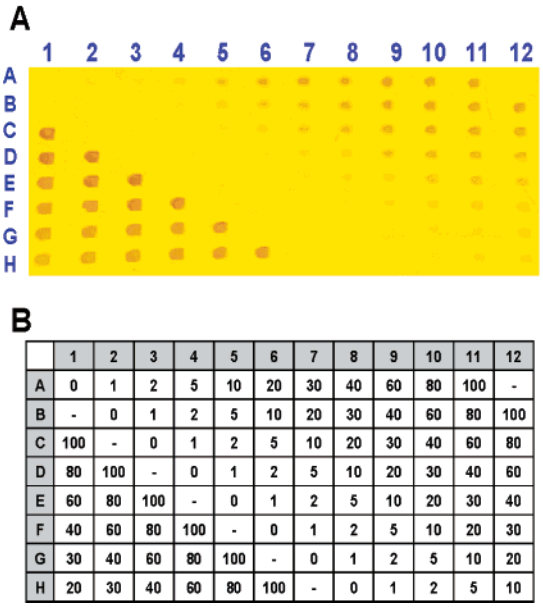

B

	1	2	3	4	5	6	7	8	9	10	11	12
A	0	1	2	5	10	20	30	40	60	80	100	-
B	-	0	1	2	5	10	20	30	40	60	80	100
C	100	-	0	1	2	5	10	20	30	40	60	80
D	80	100	-	0	1	2	5	10	20	30	40	60
E	60	80	100	-	0	1	2	5	10	20	30	40
F	40	60	80	100	-	0	1	2	5	10	20	30
G	30	40	60	80	100	-	0	1	2	5	10	20
H	20	30	40	60	80	100	-	0	1	2	5	10

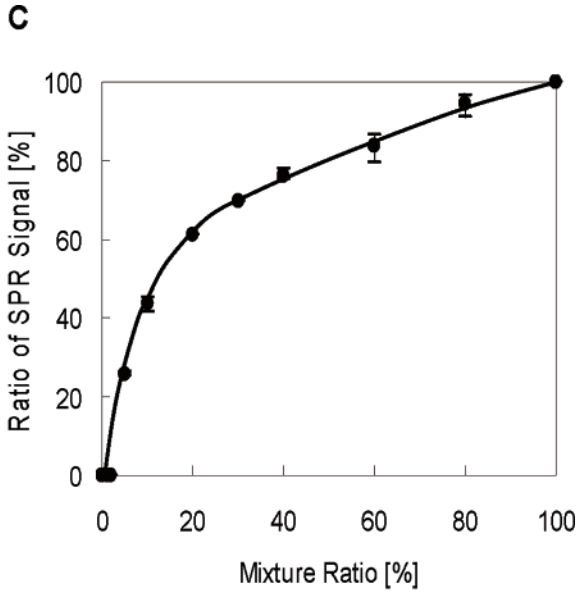

Figure 5. Quantification of the phosphorylation ratio of surface-immobilized peptide probe. (A) SPR difference image by exposure with biotinylated Zn_2L^{3+}, SA, and anti-SA on the calibration peptide array. (B) The array pattern of the various mixture ratios of probes 1 and 3 at which the peptide solutions were reacted on the chip surface during the array fabrication process. (C) The relationship between the SPR signal ratio and the phosphorylation ratio (mixture ratio); calibration curve.

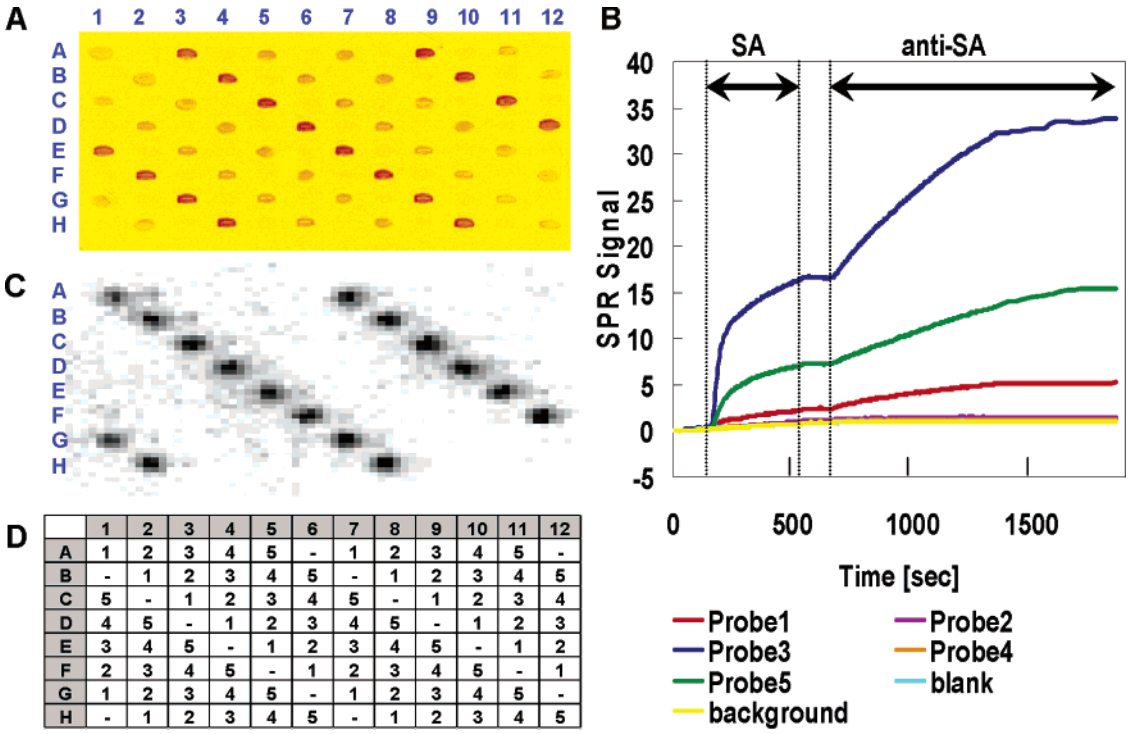

D

	1	2	3	4	5	6	7	8	9	10	11	12
A	1	2	3	4	5	-	1	2	3	4	5	-
B	-	1	2	3	4	5	-	1	2	3	4	5
C	5	-	1	2	3	4	5	-	1	2	3	4
D	4	5	-	1	2	3	4	5	-	1	2	3
E	3	4	5	-	1	2	3	4	5	-	1	2
F	2	3	4	5	-	1	2	3	4	5	-	1
G	1	2	3	4	5	-	1	2	3	4	5	-
H	-	1	2	3	4	5	-	1	2	3	4	5

Figure 6. Detection of on-chip phosphorylation of immobilized peptide by PKA. SPR difference image (A) and signal change (B) by Zn_2L^{3+} pretreatment and streptavidin exposure on the on-chip phosphorylated peptide array. (C) Autoradiography image of the peptide array, which was on-chip phosphorylated in the presence of [γ-^{32}P]-ATP. (D) The array pattern of the immobilized peptide probes.

tendency has also been observed for the calibration curve of c-Src (data not shown), though it would be necessary to establish a calibration curve for each peptide probe. In contrast, a calibration curve for the antibody detection system could not be established (data not shown). There was a threshold on the assay, and over the threshold of phosphorylation, the obtained signals were nearly saturated. These results suggest that our detection system has an advantage over the on-chip quantification of peptide phosphorylation.

Detection and Quantification of On-Chip Phosphorylation by PKA. For the on-chip phosphorylation study, we fabricated a peptide array on which probes 1−5 were immobilized with the array pattern indicated in Figure 6D. The array was exposed with PKA in the reaction buffer for 4 h, then treated with Zn_2L^{3+}, and provided for the SPR analysis. The SPR difference image and signal change in response to the exposure of 1 μg/mL SA are shown in Figure 6A and B, respectively. Probes 3 and 5 were the positive controls, which contained phosphoserine and phosphotyrosine, respectively. Probe 1, which was a variation of Kemptide, was successfully phosphorylated on the chip. Remarkably, the signals on the negative control of Kemptide (probe 2) and the c-Src substrate (probe 4) were negligible. These results suggest that probe 1 was selectively phosphorylated on the chip with PKA. The signal ratio between probes 1 and 3 was 0.60. We could calculate the phosphorylation ratio as ~20% from the calibration curve, Figure 5C. As mentioned above, the calibration curve provided an accurate quantification below 40% phosphorylation. Based on these results, we consider this assay to be in the valid range of quantification.

The array was also exposed with PKA solution containing [γ-^{32}P]-ATP and provided for the autoradiography analysis. Figure 6C shows the [γ-^{32}P]-ATP uptake results obtained with the imaging analyzer. The ^{32}P uptakes were observed only on probe 1, a result that corresponds to the SPR analysis data. Note that no ^{32}P uptake was observed on probe 3 because probe 3 had already been "100% phosphorylated".

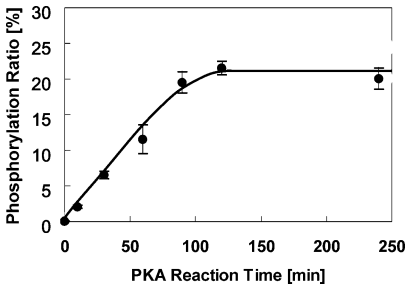

Figure 7. Phosphorylation kinetic study of the immobilized peptide probe. The phosphorylation ratios were calculated with the calibration curve, Figure 5C.

As an application of our established quantification system, we investigated the reaction kinetics of surface-immobilized peptide by PKA. Although SPR is known as a real-time analytical technique, the phosphorylations cannot be measured in real time because the assay requires some detection time (~1.5 h) as well as detection agents (Zn_2L^{3+}, SA, and anti-SA) that cannot be completely removed after the assay. We therefore prepared multiple arrays to study the reaction rate on the surface. Probes 1 and 3 were immobilized on the chip and phosphorylated by PKA for 0, 10, 30, 60, 90, 120, and 240 min. The SPR signals of probe 1 were evaluated as ratios to those of probe 3, which was 100% phosphorylated. The results are shown in Figure 7 as a time course of the phosphorylation ratio. The phosphorylation ratio was saturated at 20% in 2 h in this study.

We have previously investigated phosphorylation kinetics with PKA by mass spectrometry.[5] In the present study, the phosphorylation kinetics in solution were studied using Kemptide. The mass spectra results revealed a phosphorylation ratio of 80% at 30 min, indicating that the phosphorylation rate on the chip was much lower than that in solution. This difference may have been caused by the lower reactivity of the immobilized probe with PKA because the "immobilized" process might result in a loss of mobility of the peptide molecule, and the steric hindrance on the chip surface might affect the accessibility of PKA to the immobilized peptide.

Our results suggest that, the reaction profiles should be varied according to the peptide sequences and surface chemistries of the immobilized probes. With our established methodology, adequate probes would be selected for immobilization on the chip, and the surface chemistry would be optimized by screening the variations of tethers and cross-linkers.

CONCLUSIONS

We have proposed herein a novel detection system for on-chip phosphorylation of peptide probes with SPR imaging and a zinc(II) chelate compound. This detection method is independent of the amino acid residues so that we can detect the phosphorylation of all peptides on the array using a single-probe complex. As another advantage, this system is quantitative for phosphorylation efficiency, and the kinetics of on-chip phosphorylation can be investigated using a peptide array. This method may be a key technology for exploring peptide probes as kinase substrates and the surface chemistry of array fabrication. This technique can also be applied to high-throughput analysis of kinase activity assays and kinase expression profiling.

ACKNOWLEDGMENT

This work was supported by Project committed from New Energy and Industrial Technology Development Organization (NEDO). E.K. and T.K. would like to thank the Ministry of Education, Science, and Culture in Japan for Grant-in-Aid for Scientific Research (B) (No.15390013).

Received for review January 24, 2005. Accepted April 6, 2005.

AC050135T